

EXPERIMENTAL ACOUSTIC CHARACTERIZATION OF AUTOMOTIVE TWIN-SCROLL TURBINE

*R. Kabral*¹, *Y. El Nemr*², *C. Ludwig*³, *R. Mirlach*³, *P. Koutsovasilis*⁴, *A. Masrane*⁴,
*M. Åbom*¹

¹ Competence Center for Gas Exchange (CCGEx), KTH Royal Institute of Technology, Stockholm, Sweden, kabral@kth.se, matsabom@kth.se.

² Virtual Vehicle Research Center, Graz, Austria, yasser.elnemr@v2c2.at.

³ BMW, Munich, Germany, Email: Carlos.Ludwig@bmw.de

⁴ BorgWarner, Kirchheimbolanden, Germany, Email: PKoutsovasilis@borgwarner.com

ABSTRACT

The present paper focuses on the experimental determination of automotive twin-scroll turbine acoustic performance. The unique test-rig for automotive turbocharger acoustics at KTH CCGEx laboratory is further developed to enable testing of modern twin-scroll turbines under controlled laboratory conditions. It is shown how the passive acoustic properties of such turbines can be accurately characterized by means of an acoustic three-port formulation. Governing equations along with the new test-rig design are presented and discussed in detail. Furthermore, complementary results from the first experimental determination of twin-scroll turbine acoustic three-port data are presented.

KEYWORDS

TURBINE ACOUSTICS, TWIN-SCROLL TURBINE, TRANSMISSION LOSS, ACOUSTIC THREE-PORT.

NOMENCLATURE

A	the area of flow channel cross-section, m ²	ω	the speed of sound, m·s ⁻¹
G	single sided cross-spectrum	k	isentropic wave number, m ⁻¹
H	frequency response function	p	acoustic pressure, Pa
K	3 x 3 matrix containing complex acoustic scattering data	r	radius of pipe, m
M	the Mach number of the mean flow	s	shear wave number
Pr	Prandtl number	\mathbf{x}	3 x 1 input acoustic state vector
R	complex reflection coefficient	x	axial co-ordinate, m
T	complex transmission coefficient	\mathbf{y}	3 x 1 output acoustic state vector
TL	acoustic transmission loss, dB	γ	the ratio of specific heats
W	acoustic power, W	μ	dynamic viscosity, Pa·s
		ρ_0	the density of undisturbed medium, kg·m ⁻³
		ω	angular frequency, s ⁻¹

INTRODUCTION

In the automotive industry, turbochargers are implemented for efficiency reasons. The enthalpy of hot high pressure exhaust gas of an internal combustion (IC) engine is recovered by means of a radial inflow turbine, and used to drive the centrifugal compressor for increasing the charge air density. This leads to a better fuel conversion efficiency with low penalty of NO_x emissions. Therefore, modern IC engines, designed for higher efficiency, are equipped with turbochargers.

Presently twin-scroll type of radial turbines are being implemented more frequently in modern high efficient engine designs. The housing of the twin-scroll turbine incorporates two separated flow channels guiding exhaust gas to two different peripheral parts of the radial inflow impeller. Such design allows the separation of interfering exhaust channels of sequentially igniting cylinders, and hence result in higher turbine efficiency and better overall fuel conversion efficiency via improved scavenging effects. Moreover, because of geometrical differences between two scrolls, designed for different flow conditions, the transient response as well as maximum flow capacity are both significantly improved.

As an essential element of the IC engine exhaust system, the presence of a turbine affects both the aerodynamic as well as the acoustic fields. While a number of aerodynamic field studies are reported on the twin-scroll type turbine, and a few studies have considered single scroll turbine acoustics (Peat et al. 2006, Tiikoja et al. 2011, Veloso et al. 2012), the acoustic properties of a twin-scroll turbine have, according to the knowledge of the authors, not been investigated. It is therefore of interest to extend the previous work on acoustic characterization of single scroll turbines to twin-scroll turbines. One property of interest is the scattering of incident pressure pulses which determines the effect the unit has on the exhaust system acoustics. Moreover, such acoustic data also contains information about the small amplitude (“linear”) dynamic response of the turbine to a pulsating flow that can provide useful information for optimizing the scavenging effects or exhaust pulse energy utilization in the turbine.

In the present work, the unique test facility for acoustic testing of turbochargers at the KTH CCGEx laboratory, also used in the previous works on turbocharger acoustics (Rämmal and Åbom 2009, Tiikoja et al. 2011, Kabral et al. 2013), is further developed to enable the experimental investigation of twin-scroll turbines. The new test-rig is then used to experimentally determine acoustic performance data for an automotive twin-scroll turbine under controlled laboratory conditions.

METHOD

The turbocharger turbine is an integrated element of the full exhaust system of a modern IC engine. By assuming time invariant acoustic properties (i.e. stationary system), the turbine can be characterized separately, i.e. independently from the system, by means of acoustic n-port models (Bodén and Åbom 1995). In such models, the acoustic state of each ports of the separated element are linearly related to each other in the frequency domain as: $\mathbf{y} = \mathbf{K}\mathbf{x}$, where \mathbf{x} and \mathbf{y} denote state vectors at the input and output, respectively and \mathbf{K} is the n-port matrix.

Acoustic Three-port model

Depending on the purpose of use, different choices of acoustic state variables can be considered in the characterization. In this work the acoustic wave interaction problem is of interest, and therefore, the propagating acoustic pressure wave amplitudes is a natural choice. Assuming furthermore that the analysis is in the plane wave range, the twin-scroll turbine can be represented as a three-port described by a scattering matrix (Åbom 1991):

$$\underbrace{\begin{bmatrix} p_{a+} \\ p_{b+} \\ p_{c+} \end{bmatrix}}_y = \underbrace{\begin{bmatrix} R_{aa} & T_{ba} & T_{ca} \\ T_{ab} & R_{bb} & T_{cb} \\ T_{ac} & T_{bc} & R_{cc} \end{bmatrix}}_K \underbrace{\begin{bmatrix} p_{a-} \\ p_{b-} \\ p_{c-} \end{bmatrix}}_x. \quad (1)$$

The simplified sketch of a twin-scroll turbine with decomposed in-duct acoustic fields (waves in +/-) in its flow-channels is shown in Fig. 1.

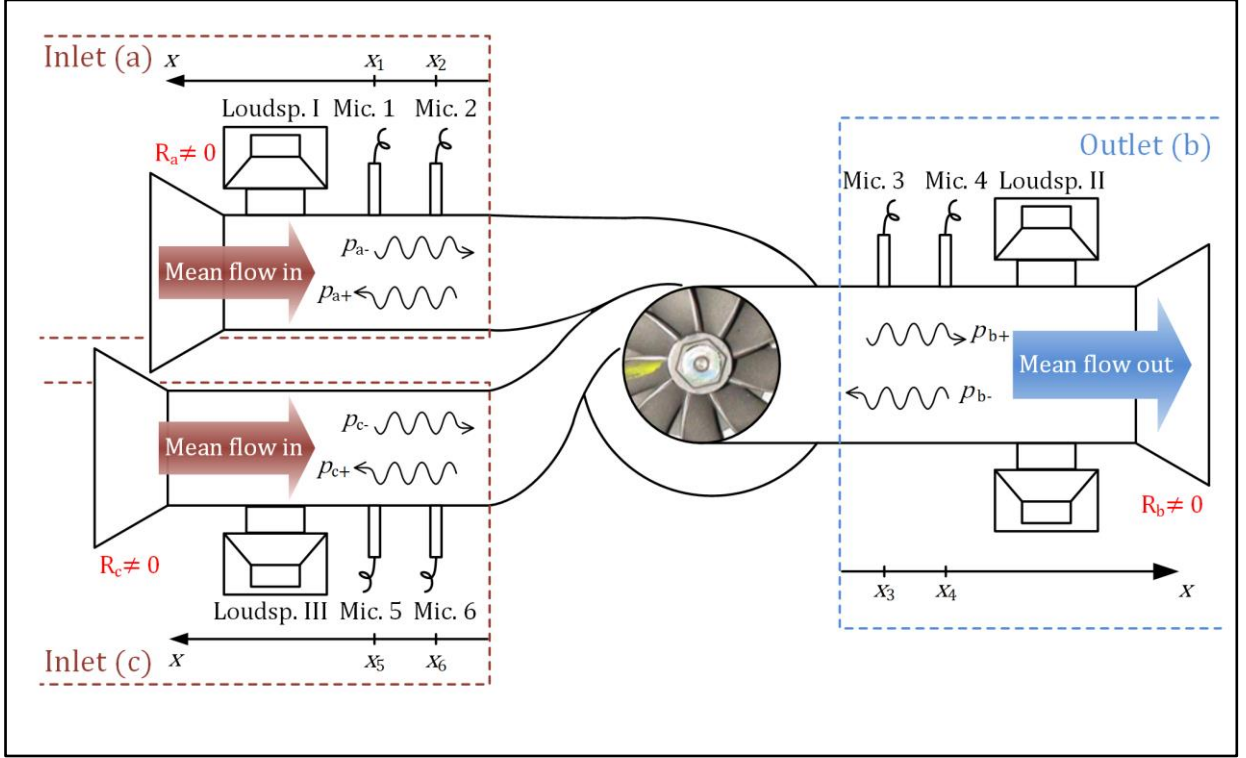


Figure 1: A simplified sketch of a twin-scroll turbine treated as an acoustic three-port.

In order to determine the nine unknown complex coefficients describing the wave interaction problem in the Eq. (1), at least nine equations i.e. three different test cases needs to be considered. Accordingly, the Eq. (1) is rewritten as:

$$\begin{bmatrix} p_{a+}^I & p_{a+}^{II} & p_{a+}^{III} \\ p_{b+}^I & p_{b+}^{II} & p_{b+}^{III} \\ p_{c+}^I & p_{c+}^{II} & p_{c+}^{III} \end{bmatrix} = \begin{bmatrix} R_{aa} & T_{ba} & T_{ca} \\ T_{ab} & R_{bb} & T_{cb} \\ T_{ac} & T_{bc} & R_{cc} \end{bmatrix} \begin{bmatrix} p_{a-}^I & p_{a-}^{II} & p_{a-}^{III} \\ p_{b-}^I & p_{b-}^{II} & p_{b-}^{III} \\ p_{c-}^I & p_{c-}^{II} & p_{c-}^{III} \end{bmatrix}. \quad (2)$$

The unknown complex scattering matrix coefficients can be found via a matrix inversion which implies the linear independency of the three test cases in Eq. (2) i.e.:

$$\det \begin{bmatrix} p_{a-}^I & p_{a-}^{II} & p_{a-}^{III} \\ p_{b-}^I & p_{b-}^{II} & p_{b-}^{III} \\ p_{c-}^I & p_{c-}^{II} & p_{c-}^{III} \end{bmatrix} \neq 0. \quad (3)$$

Such linearly independent test cases can conveniently be realized by sequentially exciting in-duct sound fields in all three branches (See Fig. 1). This is a direct extension of the so-called two-source technique used for the two-port case (Åbom 1991).

Based on the transmission coefficients in Eq. (2), the widely used quantity of acoustic transmission loss can be obtained as:

$$TL_{io} = 10 \log_{10} \frac{W_{in}}{W_{out}} = 10 \log_{10} \left[\frac{A_i \cdot \rho_o \cdot c_o \cdot (1 + M_i)^2}{|T_{io}|^2 \cdot A_o \cdot \rho_i \cdot c_i \cdot (1 + M_o)^2} \right], \quad (4)$$

where the subscript “io” denotes any pair of channels (ab, ba, ac, ca, bc, cb).

Wave decomposition

The wave decomposition of the in-duct acoustic pressure field in the fundamental plane wave frequency range is performed by employing the classical two-microphone method (Seybert and Ross 1977):

$$\begin{bmatrix} p_1 \\ p_2 \end{bmatrix} = \begin{bmatrix} e^{ik_-x_1} & e^{-ik_+x_1} \\ e^{ik_-x_2} & e^{-ik_+x_2} \end{bmatrix} \begin{bmatrix} p_- \\ p_+ \end{bmatrix}, \quad (5)$$

where

$$k_{\pm} = \frac{\omega}{c_0(1 \pm M)}. \quad (6)$$

In Eq. (5) the time dependence of $i\omega t$ and isentropic wave propagation are assumed. The opposite propagating complex wave amplitudes can be found by performing the matrix inverse operation (Eq. (5)) which implies another linear independency condition:

$$\det \begin{bmatrix} e^{ik_-x_1} & e^{-ik_+x_1} \\ e^{ik_-x_2} & e^{-ik_+x_2} \end{bmatrix} \neq 0 \Rightarrow (x_2 - x_1)(k_- + k_+) \neq 2n\pi, \quad n = 1, 2, \dots \quad (7)$$

By implementing the Eq. (6), the condition (Eq. (7)) is re-written as:

$$\frac{\omega(x_2 - x_1)}{c_0(1 - M^2)} \neq \pm n\pi. \quad (8)$$

Although, Eq. (5) is solvable when the linear independency condition (Eq. (7)) is satisfied, the sensitivity to errors is very high in the vicinity of half a wave length. By investigating different type of errors (Åbom and Bodén 1988) it was suggested that the frequency range should be limited to:

$$0.1\pi < \frac{\omega(x_2 - x_1)}{c_0(1 - M^2)} < 0.8\pi. \quad (9)$$

In high-speed flow-ducts pressure fluctuation, caused by the local turbulence, can occur under microphone membranes. This “contaminates” the acoustic pressure signal. To suppress such undesirable contribution in the signal, the driving signal of the external excitation is used as a “clean” reference signal to which all measured acoustic pressure signals are correlated to. The best estimate of the acoustic pressure signal, in the least square sense, is then obtained via the frequency response function in the following form (Bendat and Piersol 2011):

$$H_{io}(f) = \frac{G_{io}(f)}{G_{ii}(f)}. \quad (10)$$

Finally, the measurement accuracy of opposite propagating waves can be further increased by using over-determination. The following function:

$$f_j = p_- e^{ik_- x_j} + p_+ e^{-ik_+ x_j} - p_j \quad (11)$$

is formulated for all microphones, and the Euclidian norm of the vector \mathbf{f} is then minimized (Fujimori et al. 1984), i.e. the least square problem is solved. This can be conveniently done by performing Moore-Penrose pseudo-inverse on the following linear equation system:

$$\begin{bmatrix} p_1 \\ p_2 \\ \dots \\ p_n \end{bmatrix} = \begin{bmatrix} e^{ik_- x_1} & e^{-ik_+ x_1} \\ e^{ik_- x_2} & e^{-ik_+ x_2} \\ \dots & \dots \\ e^{ik_- x_n} & e^{-ik_+ x_n} \end{bmatrix} \begin{bmatrix} p_- \\ p_+ \end{bmatrix}. \quad (12)$$

Visco-thermal dissipation model

In general, isentropic wave propagation is not an adequate assumption in high-speed flow-ducts, and thus visco-thermal dissipation has to be accounted for. Although, a number of models with different complexity levels have been suggested in the literature (see e.g. Howe 1995, Dokumaci 1997, and Weng et al. 2015) in the present work the classical approach, suggested by Dokumaci, is used. This means that the isentropic wave number in the Eq. (6) is modified by a propagation constant:

$$K_0 = 1 + \left(\frac{1-i}{s\sqrt{2}} \right) \left(1 + \frac{\gamma-1}{\sqrt{Pr}} \right) \quad (13)$$

in the following fashion:

$$k_{\pm} = \frac{\omega K_0}{c_0(1 \pm K_0 M)}. \quad (14)$$

The shear wave number in Eq. (13) is defined as:

$$s = r \sqrt{\frac{\rho_0 \omega}{\mu}}. \quad (15)$$

EXPERIMENTAL SETUP

The experimental work is carried out in the KTH CCGEx laboratory for fluid mechanics and acoustics. In this laboratory, the turbochargers are isolated from the IC engine and measured separately under controlled laboratory conditions on the unique test-rig for turbocharger acoustics. The results obtained from this laboratory, under controlled realistic operating conditions, are in good agreement with results obtained from on-engine measurements, and this is without any additional compensation (El Nemr et al. 2017).

Peripheral systems

In order to determine the passive acoustic three-port data (Eq. 2), the system has to be stationary i.e. the turbine operating point (OP) is kept constant throughout the acoustic measurement. This is done by controlling the OP of the turbine by means of pneumatic throttle valves at the inlet of the turbine as well as at the outlet of the compressor (See the Fig. 2). The compressed air is supplied by external compressor plant with capability of up to 500 g per second at 5.5 bar via 25 m³ stagnation tank for pressure stabilization. Moreover, the

incoming air temperature is also increased by the 18 kW electric pre-heater system to approximately 50 °C at the turbine inlet in order to avoid ice formulation at the turbine outlet due to high rate of enthalpy extraction. The oil supply for turbocharger shaft journal bearings is provided by means of purpose built oil supply system with independent pressure and temperature control. The peripheral hardware is schematized in the Fig. 2.

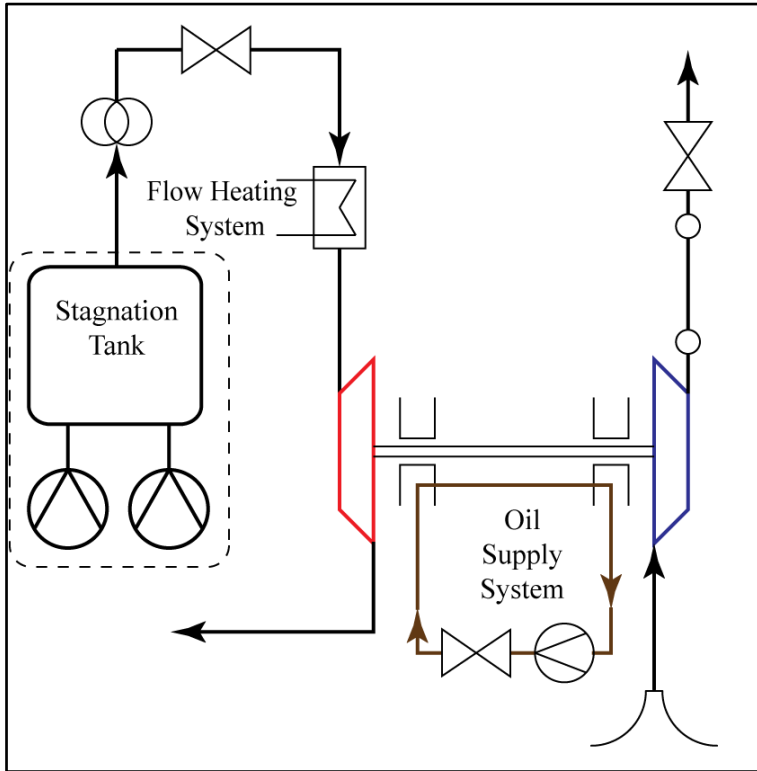


Figure 2: Peripheral hardware scheme of the KTH CCGEx turbocharger test-rig. The internal wastegate valve of the turbine is excluded from the scheme.

Test-rig for twin scroll turbines

The measurement equipment, i.e. sensors and drivers, are specified in the following Tab. 1 and complimentary layout sketch is shown in the Fig. 3.

Table 1: The list of measurement equipment with corresponding symbols in the layout sketch.

Sensor/Driver	Type or model	Measured or generated quantity	Symbol in the sketch (Fig. 3)
Condenser microphone	B&K 4941-A-011	Acoustic pressure, Pa	$p_1...p_3$
Piezoresistive abs. pressure transducer	Kulite WCT-312M	Acoustic pressure, Pa	$p_4...p_9$
Electrodynamical driver (loudspeakers)	Custom design	External excitation of acoustic pressure, Pa	$e_a...e_c$
Differential pressure sensor	NXP MPX5050DP	Quasi-static pressure, Pa	$p_{a0}-p_a; p_{b0}-p_b;$ $p_{c0}-p_c; p_{a0}^c-p_a^c, p_a^c$ $p_{b0}^c-p_b^c$
Gauge pressure sensor	Gems 2200SGA6001A3UA	Quasi-static pressure, Pa	$p_{a0}; p_{b0}; p_{c0}; p_{b0}^c$
Thermocouple	Type-K	Temperature, °C	$t_a; t_b; t_c; t_a^c; t_b^c$
Revolution counter system	Micro-epsilon turboSPEED 135	Shaft rotational frequency, RPM	RPM

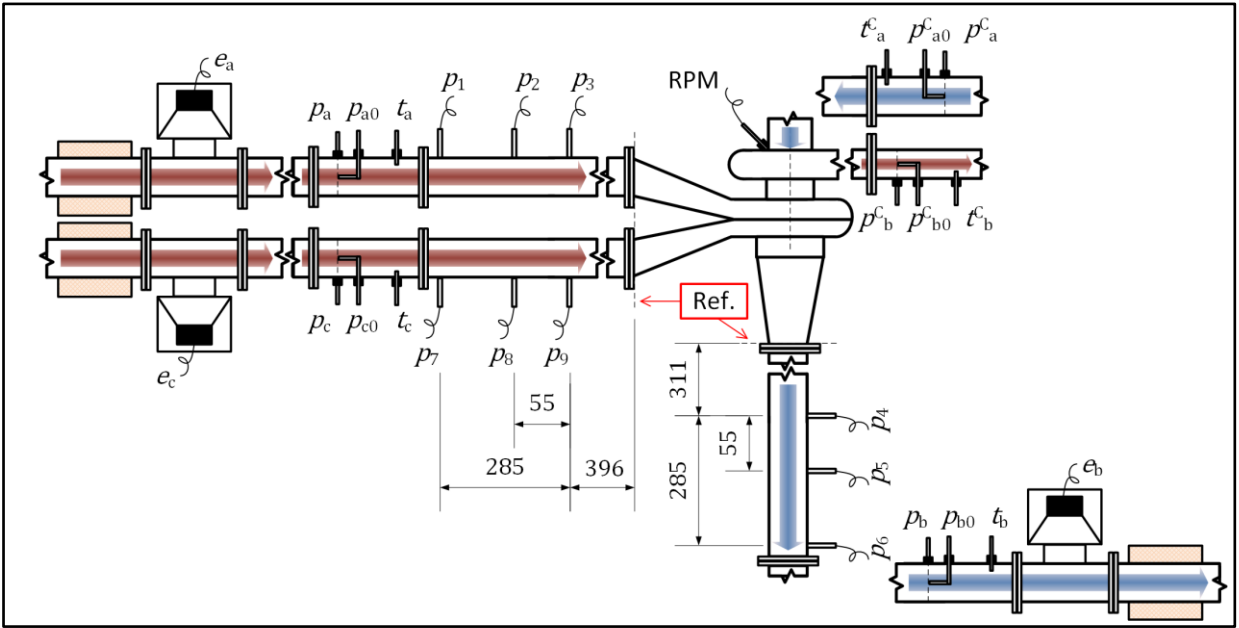


Figure 3: The location layout sketch of test rig sensors and drivers. The reference cross-sections of the determined acoustic scattering matrix data are indicated with red arrows. All lengths in mm.

The high frequency limit of plane wave propagation in the current setup is ~ 2.3 kHz. Therefore, the measurement frequency range is terminated at 2250 Hz, and corresponding intermediate distance of 55 mm between microphones is obtained by means of the Eq. 9 (See Fig. 3). Furthermore, an additional microphone is added with separation distance of 285 mm to extend the low frequency limit of measurement range. Classically, the microphone pairs are switched according to frequency band coverage (Eq. 9) while in the present work all three microphones are instead used in the over determination (Eq. **Error! Reference source not found.**) with equal weighting across the full frequency range. The external excitation is provided by means of custom built electrodynamic drivers with titanium membranes, neodymium magnet and pressure equalization channels for high pressure measurements.

The synchronous data acquisition and signal generation is performed by means of customized NI cRIO 9074 embedded control and monitoring system. Acoustic pressure signals from pressure transducers and microphones are pre-conditioned by Dewetron DAQP-Bridge-B and B&K Nexus Type 2690-A conditioners accordingly, while the generated excitation signal is amplified by means of two Zachry XP-600 professional series amplifiers. The stepped sine excitation signal is used to concentrate all the output power available to one single frequency. Moreover, three measurements on sufficiently different frequencies are performed simultaneously i.e. the external excitation with different frequencies in different turbine channels is provided simultaneously. As a consequence, the measurement time is reduced approximately three times, and thus the stability of the turbine OP during relatively long measurement time is also improved. In the present work frequency difference between simultaneous measurements is 50 Hz. Photos of the test-rig are presented in the Fig. 4.

Operating conditions

The experimental determination of the acoustic three-port data is performed on a typical modern automotive twin-scroll turbine (See Fig. 4), originating from the turbocharged R6 petrol BMW P4U engine unit equipped with direct fuel injection and Valvetronic™. The operating conditions of the turbocharger in the test-rig are set according to the reference OP of the complete engine unit (BMW P4U). Since currently the turbine air inlet temperature in the test-rig is significantly lower than the exhaust gas temperature of the engine, the

characteristic operating map, referred to as turbine map, cannot be used to accurately determine the OP. Nevertheless, on the compressor side, the realistic operating conditions are met, and the OP can be matched to reference point in the original compressor map. Therefore, the OP of the turbocharger is set for acoustic characterization by first matching the wastegate (WG) (turbine by-pass valve that is short circuiting the inlet and outlet channels of the turbine) valve position to the reference OP of the complete engine unit, and thereafter matching the compressor OP in the compressor map by means of pneumatic throttle valves (Fig. 2). The position of the WG is determined by the translation length of the WG actuator.

In addition to the operating point that is set according to the complete engine unit reference point, the comparison OP with WG position of 20 mm, corresponding to fully open position, is also measured while keeping the turbine total mass flow constant. The physical quantities determining the operating points are tabulated below (Tab. 2).

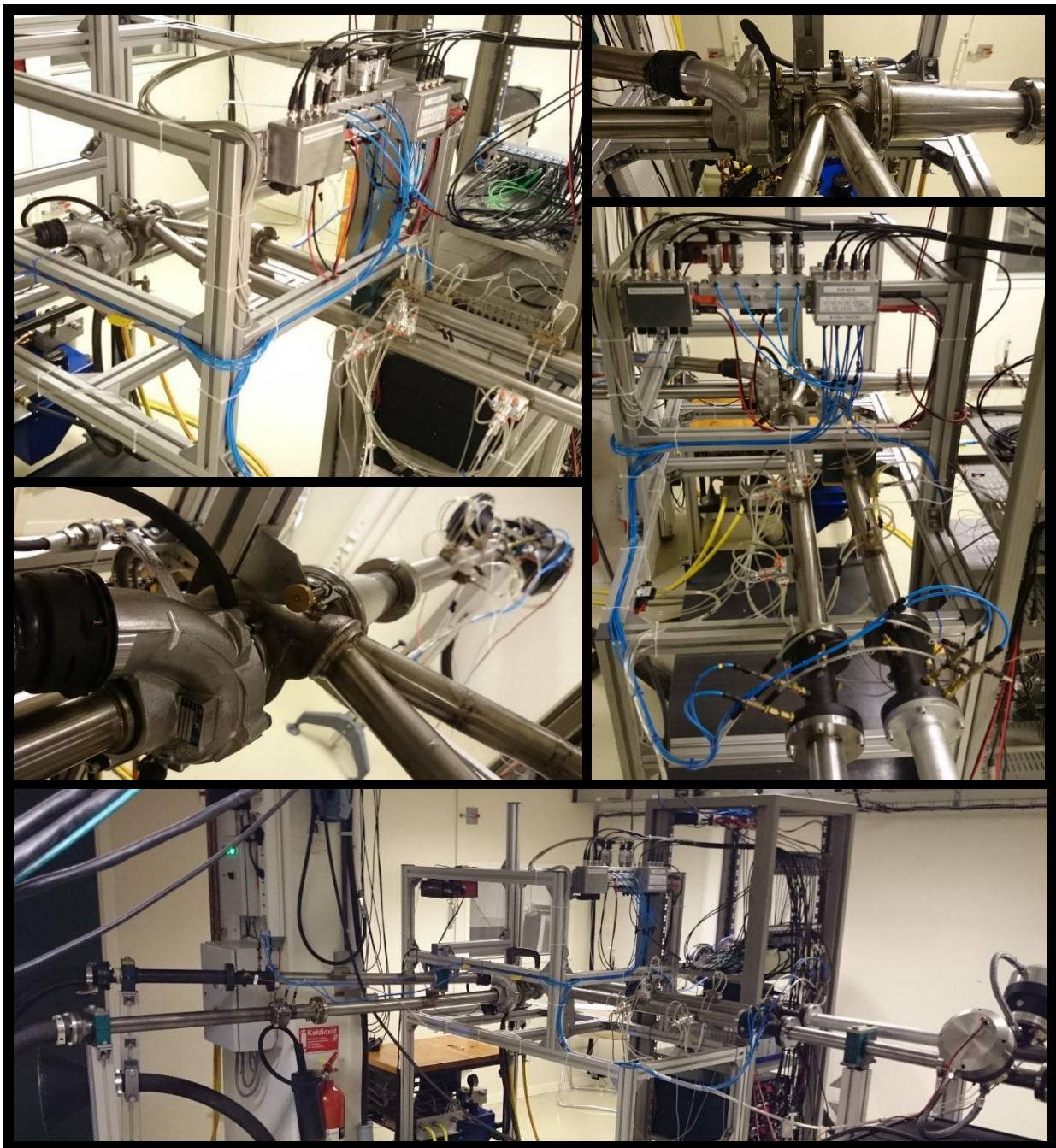


Figure 4: Photos of the unique test-rig for acoustic characterization of automotive twin-scroll turbines at the KTH CCGEx laboratory.

Table 2: The physical quantities of the turbocharger operating points during measurements.

	Ref. OP to complete engine unit OP	Comparison OP with open WG
Wastegate actuator translation length, mm	2	20
Compressor mass flow, $\text{kg}\cdot\text{s}^{-1}$	0.080	0.060
Compressor pressure ratio (total to total)	1.61	1.06
Turbine total mass flow, $\text{kg}\cdot\text{s}^{-1}$	0.200	0.200
Pressure ratio: channels a and b (total to total)	1.78	1.18
Pressure ratio: channels c and b (total to total)	1.77	1.17
Averaged shaft rotational frequency, RPM	91 166	38 780

RESULTS

The acoustic transmission loss spectra of two operating points (Tab. 2) with different wastegate positions are presented in Fig. 5.

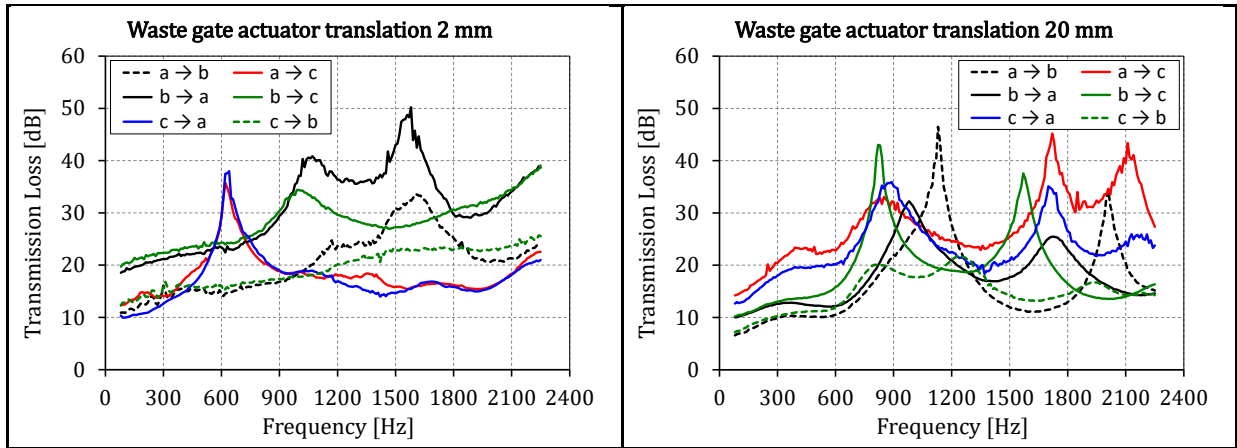


Figure 5: The spectra of acoustic transmission loss between turbine channels (a), (b) and (c) (See Fig. 1). Two different wastegate positions, determined according to the actuator translation length of 2 mm – left graph, and of 20 mm - right graph, are considered under constant total mass flow conditions (See Tab. 2).

In general the quality of the results (Fig. 5 and 6) is remarkably good. The acoustic transmission loss peak values are reaching as high as 50 dB while the broadband level remains > 10 dB (Fig. 5 left graph), thus having a significant impact to the exhaust system acoustic performance. Furthermore, the opening of the wastegate valve causes noticeable change in the character of the TL spectra (Fig. 5 left graph) by making narrowband peaks more pronounced while lowering the broadband level (Fig. 5 right graph), except the TL between two inlets. In addition, the acoustic transmission between the non-symmetrical inlet channels unpredictably remains the same regardless the propagation direction (Fig. 5 left graph).

The reflection coefficient spectra of the turbine inlets (a) and (c) with different wastegate positions (Tab. 2) are presented in the Fig. 6.

The expected dominant exhaust gas flow pulsation frequency in the turbine inlet channel is half of the engine firing frequency with its first following harmonics. The corresponding engine rotational frequency is ~ 2000 RPM which results 50 Hz (three cylinders per one turbine inlet), 100 Hz and 150 Hz of first three harmonics. Although the current measurement range starts from 80 Hz, it can be seen from the Fig. 6 left graph that in general the linear

reflection coefficient of incident low frequency (say ≤ 150 Hz) sound waves, i.e. small amplitude linear pressure pulses, is > 0.3 with steep increasing trend towards lower frequency. Predictably, the reflection coefficient magnitude in this low frequency range drops significantly by opening the WG valve, and thus creating direct connection between inlets and outlet. However, the direction of the trend towards low frequency is not so well pronounced in this case.

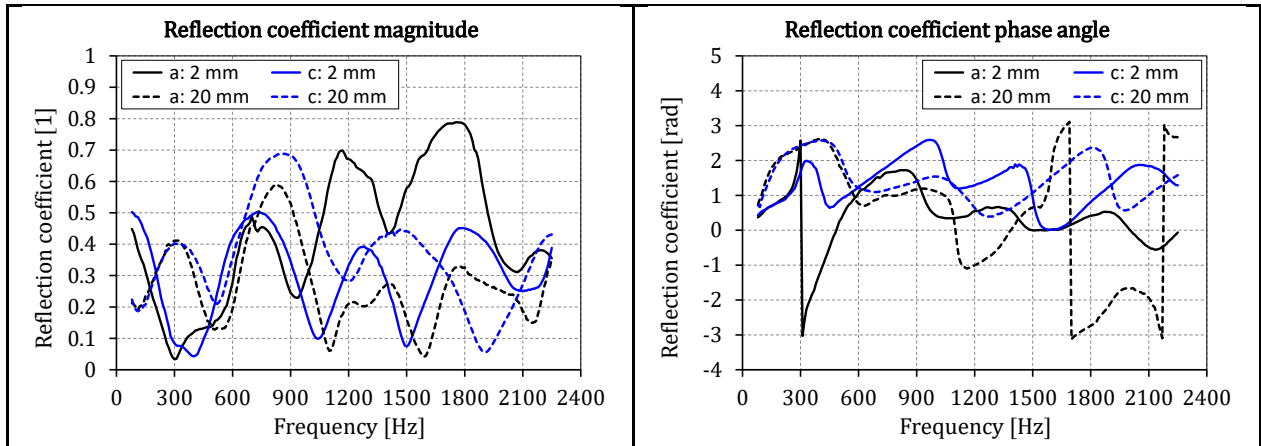


Figure 6: The reflection coefficient spectra of turbine inlets considering two different wastegate positions under constant total mass flow conditions: magnitude – left graph, and compensated phase angle – right graph. Note that the phase spectra are compensated by using the length between reference cross-section (See Fig. 3) and the location where the most significant reflection is expected to occur i.e. in case of 2 mm wastegate translation - the tongue of the turbine scroll, and in case of 20 mm - the location of the wastegate side branch.

A noticeable difference exists between two inlet channels in the frequency range above 1 kHz in case of WG valve opening of 2 mm (Fig. 6 left graph). Opening the WG valve has larger impact on the inlet (a) with significantly higher reflection coefficient value compared to the inlet channel (c) (Fig. 6 left graph).

In order to remove a very steep trend from the reflection coefficient phase angle results, the reflection coefficient phase angles are compensated in the Fig. 6 right graph by assuming corresponding length of straight pipe from the reference cross-section (See the Fig. 3) to the cross-section where the most significant reflection is expected to occur. In case of 2 mm of WG opening, i.e. almost closed, it is the turbine scroll tongue location, and in case of 20 mm, it is the cross-section of the WG side branch. As can be seen from the Fig. 6 right graph the resulting reflection coefficient “wrapped” phase spectra have no significant trends. Similarly to the reflection coefficient magnitude, the inlet channel (a) compensated phase angle has largest change between two WG positions.

CONCLUSIONS

In the present work the acoustic frequency response to incident sound waves, in this case the three-port scattering matrix, of an automotive twin-scroll turbine is experimentally determined. This is an extension of previous works (Rämmäl and Åbom 2009, Tiikoja et al. 2011, Kabral et al. 2013) concerning accurate measurements of turbo-charger acoustics, which only have covered two-ports (one inlet/outlet) configurations. By presenting and discussing the measurement methodology and test-rig design in detail it is shown how high quality data can be experimentally obtained under controlled laboratory conditions. The experimental determination of turbine acoustic data from on-engine test rigs have proved to be challenging (Peat et al. 2006). Therefore, building a dedicated acoustic turbo-charger test rig as is described in the present paper is a way to secure high quality data, which is nowadays

essential in order to validate numerical models both reduced order models (Veloso 2012) and more advanced models (Sundström 2017).

Also the first results of measurements on a twin-scroll turbine are presented and briefly discussed in the paper. It can be noted that the test are not done at the normal operating conditions of the turbine. This is not considered a problem since the data will be used for model validation. In addition one can consider to scale the data from the rig to transfer the results to a corresponding normal operating case. Based on the passive data, the reflection-free sound generation of the twin-scroll turbine, i.e. the source data independent of the coupled duct system, can further be experimentally determined as the passive data test procedure also characterizes the test-rig response. The reflection-free source data can be extracted from total measured in-duct sound field by direct extension of the complete two-port theory presented in previous works (Holmberg 2011, Kabral 2013).

ACKNOWLEDGEMENTS

This work was accomplished at KTH CCGEx in Stockholm, Sweden in close co-operation with VIRTUAL VEHICLE Research Center in Graz, Austria. The authors would like to acknowledge the financial support of the COMET K2 - Competence Centers for Excellent Technologies Programme of the Austrian Federal Ministry for Transport, Innovation and Technology (bmvit), the Austrian Federal Ministry of Science, Research and Economy (bmwfw), the Austrian Research Promotion Agency (FFG), the Province of Styria and the Styrian Business Promotion Agency (SFG).

The authors would furthermore like to express their thanks to their supporting industrial and scientific project partners, namely BMW, BorgWarner and the Inst. of IC engines (IVT).

REFERENCES

- Åbom, M., (1991). "Measurement of the Scattering-Matrix of Acoustical Two-Ports," *Mechanical Systems and Signal Processing* 5(2):89-104.
- Åbom, M., Bodén, H., (1988). *Error analysis of two-microphone measurements in ducts with flow*. *Journal of the Acoustical Society of America*, 83(6):2429–2438.
- Bendat, J. S., Piersol, A. G., (2011). *Random data: Analysis and measurement procedures*. New York : Wiley.
- Bodén, H., Åbom, M., (1995). Modelling of Fluid Machines as Sources of Sound in Duct and Pipe Systems. *Acta Acustica*, 3:1-12, 1995.
- Dokumaci, E. (1997). A note on transmission of sound in a wide pipe with mean flow and viscothermal attenuation. *Journal of Sound and Vibration*, 208(4):653-655.
- El Nemr, Y., Veloso, R., Girstmair, J., Kabral, R., Åbom, M., Schutting, E., Dumböck, O., Ludwig, C., Mirlach, R., Panagiotis, K., Masrane, A., (2017). *Experimental investigation of transmission loss in an automotive turbocharger compressor under ideal and real engine operating conditions*. Proc. of 12th European Conf. on Turbomachinery Fluid dynamics & Thermodynamics ETC12, April 3-7, Stockholm, Sweden.
- Fujimori, T., Sato, S., Miura, H., (1984). An automated measurement system of complex sound pressure reflection coefficients. *Proc. of InterNoise 84*, 1009-1014.
- Howe M.S., (1995). *The damping of sound by wall turbulent shear layers*. *The Journal of the Acoustic Society of America*, 98(3):1723-1730, doi:10.1121/1.414408.
- Kabral, R., Rämmal, H., Åbom, M., (2013). *Acoustical Methods for Investigating Turbocharger Flow Instabilities*. SAE Technical Paper 2013-01-1879, doi:10.4271/2013-01-1879.
- Peat, K. S., Torregrosa, A. J., Broatchb, A., Fernández, T., (2006). *An investigation into the passive acoustic effect of the turbine in an automotive turbocharger*. *Journal of Sound and Vibration*, 295:60-75.

- Rämmal, H. and Åbom, M., (2009). *Experimental Determination of Sound Transmission in Turbo-Compressors*. SAE Technical Paper 2009-01-2045, doi:10.4271/2009-01-2045.
- Seybert, A. F., Ross, D. F., (1977). Experimental determination of acoustic properties using a two-microphone random-excitation technique. *JASA*, 61(5):1362-1370.
- Sundström, E., Mihaescu, M., Giachi, M., Belardini, E., Michelassi, V., (2017). *Analysis of Vaneless Diffuser Stall Instability in a Centrifugal Compressor*. Proc. of 12th European Conf. on Turbomachinery Fluid dynamics & Thermodynamics ETC12, April 3-7, Stockholm, Sweden.
- Tiikoja, H., Rämmal, H., Åbom, M., and Bodén, H., (2011). *Sound Transmission in Automotive Turbochargers*. SAE Technical Paper 2011-01-1525, doi:10.4271/2011-01-1525.
- Veloso, R., Elnemr, Y., Reich, F., Allam, S., (2012,). *Simulation of Sound Transmission through Automotive Turbochargers*. SAE Technical Paper 2012-01-1560, doi:10.4271/2012-01-1560.
- Weng C., Boij S., Hanifi A., (2015). *On the calculation of the complex wavenumber of plane waves in rigid-walled low-Mach-number turbulent pipe flows*. *Journal of Sound and Vibration*, 354:132-153, doi:10.1016/j.jsv.2015.06.013.